

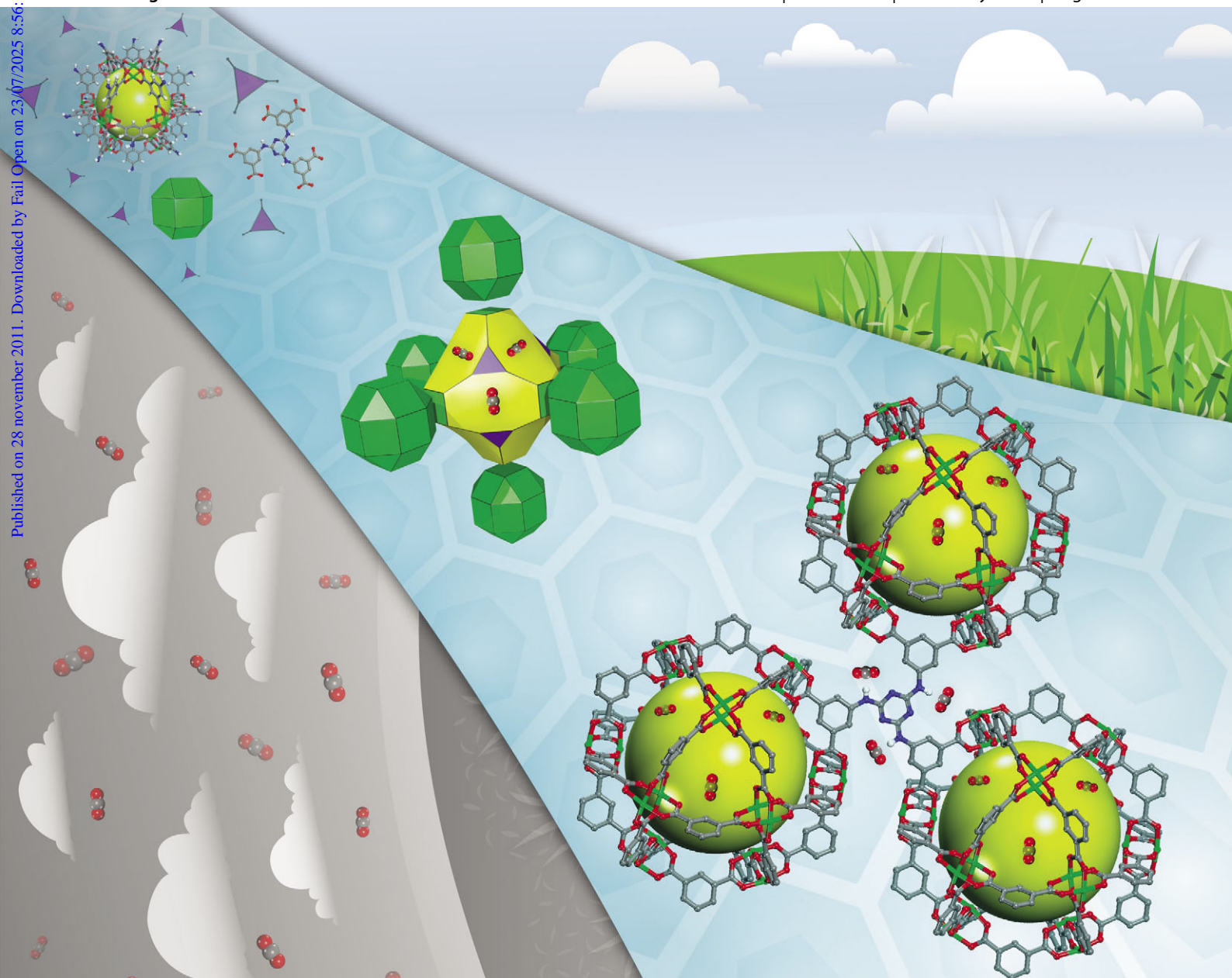
# ChemComm

Chemical Communications

[www.rsc.org/chemcomm](http://www.rsc.org/chemcomm)

Volume 48 | Number 10 | 1 February 2012 | Pages 1325–1608

Published on 28 November 2011. Downloaded by Fail Open on 23/07/2025 8:56:12.



Emerging Investigators Issue 2012

ISSN 1359-7345

RSC Publishing

**COMMUNICATION**

Eddaoudi *et al.*

The unique rht-MOF platform, ideal for pinpointing the functionalization and CO<sub>2</sub> adsorption relationship



1359-7345(2012)48:10;1-H

Cite this: *Chem. Commun.*, 2012, **48**, 1455–1457

www.rsc.org/chemcomm

## COMMUNICATION

The unique *rht*-MOF platform, ideal for pinpointing the functionalization and CO<sub>2</sub> adsorption relationship†‡Ryan Luebke,<sup>a</sup> Jarrod F. Eubank,<sup>b</sup> Amy J. Cairns,<sup>a</sup> Youssef Belmabkhout,<sup>a</sup> Lukasz Wojtas<sup>b</sup> and Mohamed Eddaoudi<sup>\*ab</sup>

Received 25th September 2011, Accepted 3rd November 2011

DOI: 10.1039/c1cc15962c

The uniqueness of the *rht*-MOF platform, based on the singular (3,24)-connected net, allows for the facile design and synthesis of functionalized materials for desired applications. Here we designed a nitrogen-rich trefoil hexacarboxylate (trigonal tri-isophthalate) ligand, which serves to act as the trigonal molecular building block while concurrently coding the formation of the targeted truncated cuboctahedral supermolecular building block (*in situ*), and enhancing the CO<sub>2</sub> uptake in the resultant *rht*-MOF.

Carbon dioxide is considered to be the main anthropogenic contributor to the greenhouse gas effect, as it is allegedly responsible for 60% increase in atmospheric temperature, commonly referred to as “global warming”.<sup>1</sup> In order to maintain a desired environmental sustainability for future generations, it is becoming critical to develop effective methods for the capture and use of CO<sub>2</sub> from stationary post-combustion effluents, such as flue gas, as well as from vehicle emissions.<sup>2</sup>

The current dominant industrial carbon capture process, based on gas absorption using alkanolamine solutions, is energy intensive and costly for general deployment.<sup>3</sup> Alternatively, inspired by amine scrubbing technology, it is anticipated that selective CO<sub>2</sub> sorption at relatively low pressures on prospective high surface area porous solids enclosing amine functionalities can be the appropriate approach and the practical alternative solution to address the carbon capture challenge.<sup>3,4</sup>

Metal-organic frameworks (MOFs) have emerged as potentially suitable materials for carbon capture due to their thermal and chemical stability, permanent porosity with extra-high surface areas, modular and tunable character.<sup>5</sup> Toward a made-to-order MOF suitable for superior carbon capture, it is critical to assess the impact of cavity size, shape, polarity and functionality on sorption energetics of CO<sub>2</sub>. A functional MOF encompassing

cavities and windows decorated with Lewis basic sites (*e.g.*, amino groups and triazine nitrogen atoms) could potentially lead to enhanced CO<sub>2</sub> sorption energies.<sup>6</sup> The unique features of our *rht*-MOF platform,<sup>7</sup> the singular MOF for the combination of trigonal molecular building blocks (MBBs) (3-connected node) and truncated cuboctahedral supermolecular building blocks (SBBs) (24-connected rhombicuboctahedral node) (Fig. 1a), offer the potential to tailor the MOF structure and properties, and gain better insight on the structure–properties relationship.

The exceptional versatility of our SBB-based approach and the uniqueness of the *rht*-MOF platform, combined with the vast library of organic syntheses, allow for facile incorporation of multiple [desired/targeted] functions into the same structure/material. To execute this approach, we designed and synthesized a highly functionalized organic trefoil-like, trigonal tri-isophthalate (*i.e.*, hexacarboxylate) ligand, 5,5',5''-(1,3,5-triazine-2,4,6-triyltriamino)tris-isophthalate hexasodium {5,5',5''-(1,3,5-triazine-2,4,6-triyltriamino)tris-1,3-benzenedicarboxylate

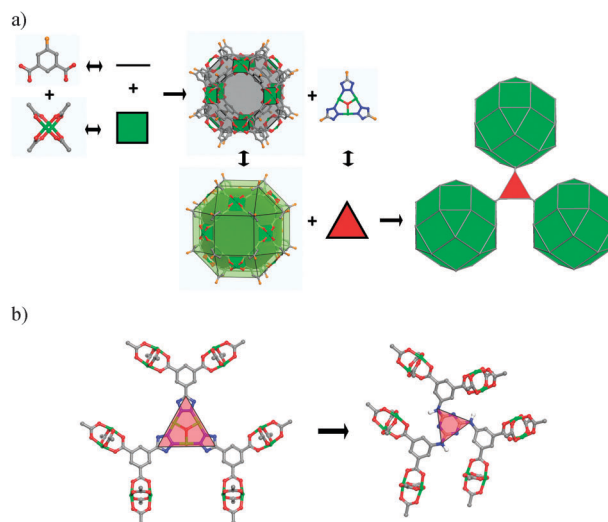


**Fig. 1** *rht*-MOFs: (a) Scheme for formation, from 5-R-1,3-BDC and paddlewheel MBBs, of the *tez*-SBB, which is concomitantly linked [3×] to a Cu<sub>3</sub>O(N<sub>4</sub>CR)<sub>3</sub> MBB periodically to form the 3D *rht*-MOF; (b) trigonal core (red triangle) can be deliberately substituted by an organic core (*e.g.* tri-substituted triazine), resulting in a trefoil-type organic ligand where the analogous isophthalate termini serve to form the paddlewheel MBBs of the SBB. Only the amine hydrogen atoms are included for clarity.

<sup>a</sup> KAUST Advanced Membranes & Porous Materials Center, 4700 King Abdullah University of Science and Technology, Thuwal 23955-6900, Kingdom of Saudi Arabia. E-mail: mohamed.eddaoudi@kaust.edu.sa

<sup>b</sup> Department of Chemistry, University of South Florida, 4202 East Fowler Avenue (CHE 205), Tampa, FL 33620, USA

† This article is part of the ChemComm ‘Emerging Investigators 2012’ themed issue.

‡ Electronic supplementary information (ESI) available: Experimental procedures, PXRD, sorption, and single-crystal X-ray diffraction data. CCDC 846266. For ESI and crystallographic data in CIF or other electronic format see DOI: 10.1039/c1cc15962c

hexasodium} ( $\text{Na}_6\text{L}$ ) (Fig. S1, ESI†),<sup>8</sup> where the trigonal core is a nitrogen-rich, tri-substituted triazine core, and an amine functional group is introduced between the core and isophthalate termini (Fig. 1b).

Indeed, reaction between  $\text{Na}_6\text{L}$  and copper tetrafluoroborate under solvothermal conditions§ results in the targeted **rht**-MOF. Single-crystal X-ray diffraction reveals a formula unit of  $[\text{Cu}_3\text{L}(\text{H}_2\text{O})_3(\text{solvent})]_n$ , (**rht**-MOF-7) indicating the predicted structure, analogous/isoreticular to the original **rht**-MOF, hereby denoted as our **rht**-MOF-1.<sup>7</sup> In the crystal structure of **rht**-MOF-7, each central triazine core is covalently linked through amine moieties at the 2,4,6-positions (3-connected) to the 5-position of each isophthalate terminus. The isophthalate terminus allows formation, *in situ*, of the truncated cuboctahedral (24 functionalized isophthalate ligands connected by 12 copper dimer centers,  $\text{Cu}_2(\text{O}_2\text{CR})_4$  paddlewheels) SBB (**tcz**, [3<sup>8</sup>.4<sup>18</sup>]),<sup>9</sup> where the 5-position of each bridging isophthalate moiety (bent, 120° angle) lies exactly on the vertices of a rhombicuboctahedron<sup>10</sup> (**rco**),<sup>9</sup> the [24-connected] vertex figure necessary for **rht**-MOFs (Fig. 1a).<sup>7</sup>

The packing of the rhombicuboctahedra results in additional extra-large cavities, primarily elongated truncated cube (**tcu**, [3<sup>8</sup>.8<sup>6</sup>]) cavities and augmented rhombic dodecahedral (**rdo-a**, [3<sup>8</sup>.4<sup>6</sup>.8<sup>12</sup>]) cavities (Fig. 2b–d).<sup>9</sup> The reduced dimension of the triangular organic core in **rht**-MOF-7 (*vs.* inorganic in **rht**-MOF-1) (Fig. 1b) has resulted in the reduction of the **tcu** and **rdo-a** cavities (10.4 and 17.8 Å, respectively) compared to **rht**-MOF-1 (12.1 and 20.2 Å, respectively), though, as expected, the **tcz** cavity size remains the same (~16 Å inner diameter). Correspondingly, the windows of the **rdo-a** and **tcu** cavities are also smaller, *i.e.*, 6.4 Å *vs.* 7.4 Å in **rht**-MOF-7 and -1, respectively. It is important to note that, due to the ligand design/function in **rht**-MOF-7, the windows/apertures allowing access to those cavities are decorated with amine groups. Accordingly, the reduced size of **tcu** and **rdo-a** cavities in **rht**-MOF-7, combined with exposed amines and a more polarized core, offers the potential to explore the effects of pore size and functionality on sorbates of interest, especially  $\text{CO}_2$ .<sup>4,6</sup>

The potential accessible free volume for **rht**-MOF-7 was estimated from the X-ray crystal structure to be 70%, by summing voxels more than 1.2 Å away from the framework. Sorption studies confirm the permanent microporosity of **rht**-MOF-7, as evidenced by the fully reversible type I Argon sorption isotherm (Fig. S3a, ESI†). The apparent Langmuir surface area for **rht**-MOF-7 was estimated to be 2170 m<sup>2</sup> g<sup>-1</sup> which, as anticipated, was lower than **rht**-MOF-1 due to the reduced size of the **tcu** and **rdo-a** cavities in **rht**-MOF-7. The calculated total free pore volume was estimated to be 0.76 cm<sup>3</sup> g<sup>-1</sup>. The pore size distribution, calculated from the argon isotherm, shows the three expected pore sizes with estimated diameters of 16.6, 10.3, and 8.1 Å (Fig. S3b, ESI†).

The readily exposed amines and a more polarized core (triazine), combined with the reduced size of **tcu** and **rdo-a** cavities in **rht**-MOF-7, are attractive features for evaluating the impact of pore size, shape and functionality on  $\text{CO}_2$  sorption energetics and uptake. Accordingly,  $\text{CO}_2$  sorption experiments were carried out at various temperatures on **rht**-MOF-7 and on the parent **rht**-MOF-1, as a reference compound. The maximum uptake was measured at 273 K and 1 bar and found to be higher for **rht**-MOF-7 (6.52 *vs.* 4.40 mmol g<sup>-1</sup> for **rht**-MOF-1) (Fig. 3).

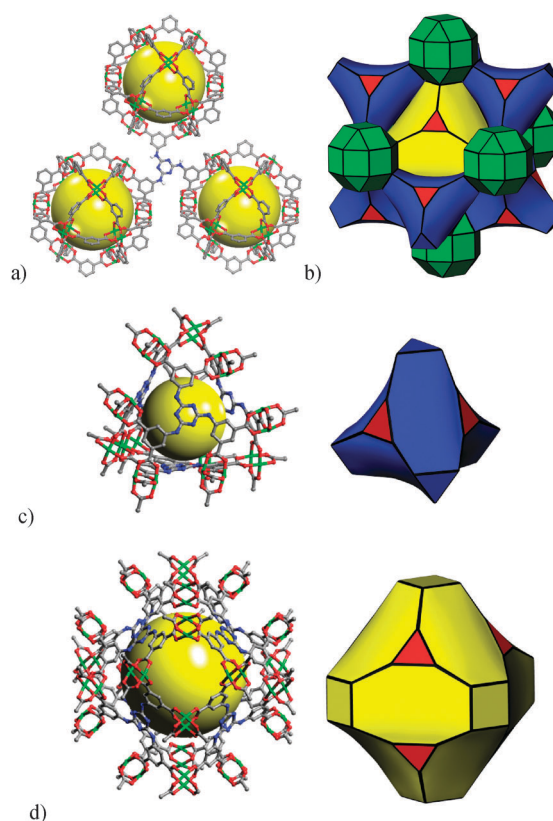


**Fig. 2** Selected fragments from the single-crystal structure of **rht**-MOF-7: (a) One triazine-core ligand surrounded by three **tcz** cavities/SBBs which, (b) when modified at the 5-position of the 1,3-BDC units, also serve as the **rco** vertex figure (green polyhedron) in **rht** (tiling representation); (c) one **tcu** cavity and the corresponding tile; (d) one **rdo-a** cavity and the corresponding tile. The yellow sphere represents the largest van der Waals sphere that will fit in the cavity. The triangular vertex figure is indicated in red. Hydrogen atoms and solvent molecules have been omitted for clarity. C = gray; N = blue; O = red; Cu = green.

The isosteric heat of  $\text{CO}_2$  adsorption,  $Q_{\text{st}}$ , for both compounds was calculated from the Clausius–Clapeyron equation using adsorption data collected at temperatures between 258 and 298 K (see Fig. S3, ESI†). The  $Q_{\text{st}}$  for  $\text{CO}_2$  was found to be relatively higher for **rht**-MOF-7 at low loading in comparison to **rht**-MOF-1 (*i.e.* 44.7 *vs.* 32.5 kJ mol<sup>-1</sup> at zero loading), followed by convergence into a pseudo-plateau at relatively higher uptakes.

It should be mentioned that the accuracy of the  $Q_{\text{st}}$  determination for **rht**-MOF-7 and **rht**-MOF-1 was confirmed by the established linearity of  $\text{CO}_2$  isosters (Fig. S4 and S5, ESI†) for the entire studied range of  $\text{CO}_2$  loadings. The relatively high  $Q_{\text{st}}$  at low loading for **rht**-MOF-7 is in the same range as other amine-functionalized MOFs and is among the highest  $Q_{\text{st}}$  values recorded for sorbed  $\text{CO}_2$  on MOFs.<sup>6</sup> Enhanced  $\text{CO}_2$  interaction is key for improving selectivity toward  $\text{CO}_2$ , which is critical for gas separation and purification (*e.g.*,  $\text{CH}_4$ ,  $\text{N}_2$ ,  $\text{H}_2$ , ...).

The observed enhancement in the  $\text{CO}_2$  sorption energetics in the case of **rht**-MOF-7 is likely attributed to the combined size and surface effects pertaining to the exposed free amine groups and triazine nitrogen atoms, promoting stronger  $\text{CO}_2$  interaction with nitrogen donor groups decorating the surface of the cavities. The  $Q_{\text{st}}$  for **rht**-MOF-7 decreases at higher  $\text{CO}_2$  pressures reaching a pseudo-plateau (~24–29 kJ mol<sup>-1</sup>) and

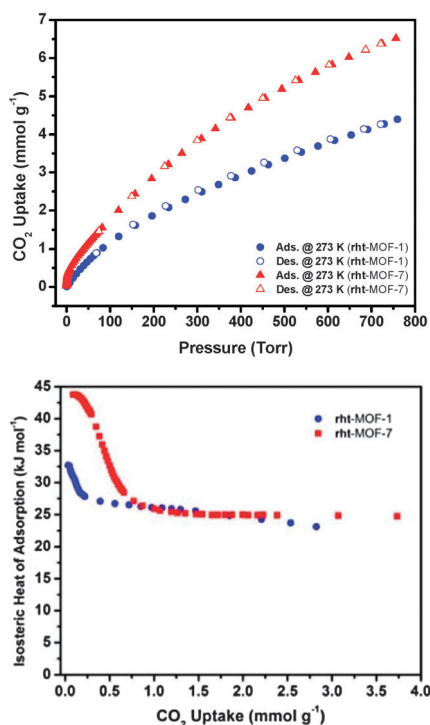


**Fig. 3** (top) CO<sub>2</sub> sorption isotherms for **rht**-MOF-1 (blue) and **rht**-MOF-7 (red); (bottom)  $Q_{st}$  for CO<sub>2</sub>, **rht**-MOF-1 (blue), **rht**-MOF-7 (red).

converges to values similar to those observed for **rht**-MOF-1 at relatively higher loading. In order to further elucidate the CO<sub>2</sub> interactions with **rht**-MOF-7, we completed a study pertaining to the energetics of CO<sub>2</sub> adsorption using multiple sites Langmuir Model (MSL). The ultimate objective of this analysis is to identify various available energy sites for CO<sub>2</sub> adsorption in **rht**-MOF-7.

The ideal fit was obtained when applying the dual site Langmuir model (DSL), as shown in Fig. S6 (ESI<sup>†</sup>), indicating the presence of two clearly distinct energetic sites. The deduced DSL fit parameters (Table S2, ESI<sup>†</sup>) were used to generate adsorption isotherms pertaining to each independent adsorption site (Fig. S7 and S8, ESI<sup>†</sup>) and the resulting isotherms were then employed to calculate the corresponding  $Q_{st}$  for each site (Fig. S9, ESI<sup>†</sup>).

The aforementioned analysis confirms the presence of two isolated energetic sites for CO<sub>2</sub> adsorption. The first preferential adsorption sites around 45 kJ mol<sup>-1</sup> can be attributed to favored interactions with exposed amine and triazine moieties. The resulting promoted CO<sub>2</sub> sorption at low loading, also evidenced by the sorption isotherm steepness at lower coverage (Fig. 3a), is a highly desirable feature for CO<sub>2</sub> capture applications at reduced partial pressures. The second distinct energetic sites (~25 kJ mol<sup>-1</sup>) are dominated by pore filling, indicative of relatively weaker CO<sub>2</sub> interactions at high loading.

In contrast, applying the DSL model to the acylamide-based **rht**-MOF<sup>11</sup> reveals only sorption sites with relatively similar energies (~27 kJ mol<sup>-1</sup>), expressed by a non-converging fit for both sites with interdependent parameters. Consequently, the entire data are best fit with a single adsorption site model and suggest limited impact of the introduced amide functionality on the CO<sub>2</sub> sorption energetics at low loading (Table S3 and Fig. S10, ESI<sup>†</sup>).

The CO<sub>2</sub> sorption data and  $Q_{st}$  analysis confirm the importance of the generated close proximity between amine groups and triazine moieties in the **rht**-MOF-7. The nitrogen donor groups, decorating the relatively small triangular window apertures and thus providing peripheral high localized charged density, play a major role in the observed enhanced CO<sub>2</sub> sorption energetics at low loadings.

We have successfully used the **rht**-MOF platform to prepare a deliberately functionalized **rht**-MOF exhibiting high affinity toward CO<sub>2</sub> at lower loading as a result of a unique combination of amine and triazine moieties decorating the available high surface area, windows and pores. Further sorption studies are in progress to evaluate the particular effect of combined triazine and amine functionalization on the adsorption selectivity of acid gases (CO<sub>2</sub>, H<sub>2</sub>S, SO<sub>2</sub>, etc.) in the presence of N<sub>2</sub>, CH<sub>4</sub> and H<sub>2</sub> containing gas mixtures. Ongoing efforts are devoted to the incorporation of additional energetically favorable sites (e.g., primary and/or secondary amine functional groups) which offers potential to widen the observed higher affinity toward CO<sub>2</sub> to relatively higher CO<sub>2</sub> loading, thus permitting access to novel **rht**-MOFs with superior selectivity and uptakes for post-combustion CO<sub>2</sub> capture. The amine functionalization will be further extended to the **tcz** cavity thus augmenting the density of amine groups per unit volume.

The authors gratefully acknowledge KAUST funds.

## Notes and references

§ Crystallographic data for [Cu<sub>3</sub>(L)<sub>3</sub>(H<sub>2</sub>O)<sub>3</sub>]<sub>n</sub>, (**rht**-MOF-7): C<sub>27</sub>H<sub>12</sub>Cu<sub>3</sub>N<sub>6</sub>O<sub>15</sub>,  $M = 353.22$ , tetragonal,  $I4/m$ ,  $Z = 16$ ,  $a = 26.6700(3) \text{ \AA}$ ,  $c = 38.042(1) \text{ \AA}$ ,  $V = 27058.6(8) \text{ \AA}^3$ ,  $D = 0.836 \text{ g cm}^{-3}$ ,  $T = 100(2) \text{ K}$ ,  $N_{\text{Ref}} = 44425/10968$ ,  $R_{\text{int}} = 0.11$ ,  $R_{[I > 2\sigma(I)]} = 0.055$ ,  $wR_{[I > 2\sigma(I)]} = 0.116$ ,  $R_{\text{all data}} = 0.094$ ,  $wR_{\text{all data}} = 0.124$ . CCDC 846266. Data were treated with the SQUEEZE procedure implemented in the Platon program.<sup>12</sup>

- 1 A. J. Yamakasi, *J. Chem. Eng. Jpn.*, 2003, **36**, 361–375.
- 2 D. J. Hofmann, J. H. Butler and P. P. Tans, *Atmos. Environ.*, 2009, **43**, 2084–2086.
- 3 A. Sjoström and H. Krutka, *Fuel*, 2010, **89**, 1298–1306.
- 4 A. Sayari and Y. Belmabkhout, *J. Am. Chem. Soc.*, 2010, **132**, 6312–6314; V. Zelenak, D. Halamova, L. Gaberova, E. Bloch and P. Llewellyn, *Microporous Mesoporous Mater.*, 2008, **116**, 358–364; R. Vaidhyanathan, S. S. Iremonger, G. K. H. Shimizu, P. G. Boyd, S. Alavi and T. K. Woo, *Science*, 2010, **330**, 650–653; Y. Belmabkhout and A. Sayari, *Adsorption*, 2009, **15**, 318–328.
- 5 *Metal-Organic Frameworks: Design and Application*, ed. L. MacGillivray, WILEY-VCH Verlag GmbH & Co. KGaA, Weinheim, 2010, and references therein.
- 6 J. An, S. J. Geib and N. L. Rosi, *J. Am. Chem. Soc.*, 2010, **132**, 38–39; B. Arstad, H. Fjellvåg, K. O. Kongshaug, O. Swang and R. Blom, *Adsorption*, 2008, **14**, 755–762; S. Couck, J. F. M. Denayer, G. V. Baron, T. Remy, J. Gascon and F. Kapteijn, *J. Am. Chem. Soc.*, 2009, **131**, 6326–6327; P. L. Llewellyn, S. Bourrelly, C. Serre, M. D. Vimont, L. Hamon, G. D. Weireld, J. S. Chang, D. Y. Hong, Y. K. Hwang, S. H. Jung and G. Férey, *Langmuir*, 2008, **24**, 7245–7250.
- 7 F. Nouar, J. F. Eubank, T. Bousquet, L. Wojtas, M. J. Zaworotko and M. Eddaoudi, *J. Am. Chem. Soc.*, 2008, **130**, 1833–1835.
- 8 R. B. Conrow and S. Bernstein, *Tri-Substituted Triazines. U.S. Patent 4,183,929*, 1980.
- 9 M. O’Keeffe, M. A. Peskov, S. J. Ramsden and O. M. Yaghi, *Acc. Chem. Res.*, 2008, **41**, 1782–1789.
- 10 M. Eddaoudi, H. Li and O. M. Yaghi, *J. Am. Chem. Soc.*, 2000, **122**, 1391–1397.
- 11 B. Zheng, J. Bai, J. Duan, L. Wojtas and M. J. Zaworotko, *J. Am. Chem. Soc.*, 2011, **133**, 748–751.
- 12 (a) T. L. Spek, *Acta Crystallogr., Sect. A: Found. Crystallogr.*, 1990, **46**, 194–201; (b) T. L. Spek, *Acta Crystallogr.*, 1990, **A46**, c34.